AIAA JOURNAL
Vol. 31, No. 10, October 1993

Optimal Placement of Active Elements in Control Augmented Structural Synthesis

A. E. Sepulveda,* I. M. Jin,† and L. A. Schmit Jr.‡
University of California, Los Angeles, Los Angeles, California 90024

A methodology for structural/control synthesis is presented in which the optimal location of active members is treated in terms of (0,1) variables. Structural member sizes, control gains, and (0,1) placement variables are treated simultaneously as design variables. Optimization is carried out by generating and solving a sequence of explicit approximate problems using a branch and bound strategy. Intermediate design variable and intermediate response quantity concepts are used to enhance the quality of the approximate design problems. Numerical results for example problems are presented to illustrate the efficacy of the design procedure set forth.

Introduction

LARGE space structures, which are very flexible due to low weight requirements, need some type of active control system to suppress vibrations and maintain stringent shape specifications.[1,2] Vibrations and shape variations can be induced by several sources, such as position maneuvers, thermal gradients, and docking procedures. Stringent shape specifications must often be satisfied to maintain pointing accuracy of optical and radar systems. Because of their low weight and large size, space structures will tend to have low frequencies and very little inherent damping. Furthermore, for the transient disturbances usually encountered, the structure remains unchanged once they are damped out; therefore, such disturbances call for active controls that enhance the damping of the structure.

For the case of space structures made of truss and frame elements, it is often appropriate to implement the control system by replacing some of the passive structural elements with active actuator elements that provide the control forces. A practical implementation of these kinds of actuators, which has been experimentally tested,[3-5] makes use of piezoelectric materials. The actuators are manufactured by stacking thin layers of piezoelectric material in a structural casing. When a control voltage is applied to the piezoelectric stack, it induces expansion of this material and thus a change in length in the active element. This induced strain has the effect of an applied control force on the structure. The control system is implemented by designing a feedback control law for the applied voltage.

The effectiveness of the control system is strongly dependent on the active element locations. In fact, the degree of controllability of the structure/control system, which depends primarily on the active element locations, will have a major influence on the efficiency of the control system and the control effort required to satisfy design requirements. Selecting the active element locations, from a discrete set of possible positions, represents a combinatorial problem that can be formulated in terms of (0,1) variables. Several techniques have been brought to bear on these kinds of problems. Reference 6 uses simulated annealing as the optimization algorithm, Lagrange multipliers techniques are used in Ref. 7, and minimum control energy criteria are employed in Ref. 8. In Refs. 9 and 10, the approach is to find optimum damper locations by optimizing damping coefficients. For the case of static loads, the problem has been treated in Refs. 11 and 12.

In this work the integrated structure/control design optimization problem is formulated as a nonlinear mathematical programming problem involving both continuous and (0,1) variables. Here a direct output feedback control law is adopted for the applied voltage. The displacement and velocity gains for each active element are then treated as independent design variables in the optimization procedure. The combinatorial aspects of the mixed-(0,1) continuous optimization are dealt with using a strategy that combines approximation concepts (based on extensive use of intermediate design variables and intermediate response quantities) and branch and bound techniques.[13]

Piezoelectric Actuators

Several kinds of active members have been studied for the implementation of control systems in large space structures, including proof mass actuators, voice coils, gas jets, and piezoelectric-based actuators.[4] Piezoelectric devices seem to be more suitable for the control of precision structures, where very small displacement requirements are to be satisfied. In this work, piezoelectric-based actuators are chosen for the integrated structural/control system synthesis.

Piezoelectric materials expand or contract in response to an electric field while maintaining elastic characteristics. This property is exploited in Ref. 4 to construct an active element in which n wafers of thickness t are stacked and wired electrically in parallel to form a single axial actuator. The mechanical model for a piezoelectric actuator can be represented by a force-deformation relation of the following form:

$$F_a = k_a(\delta + \delta_0 - \delta_V) \tag{1}$$

where F_a is the total force induced in the actuator, k_a the mechanical stiffness of the actuator, δ the elastic change in length, δ_0 the initial contraction of the piezoelectric material ($\delta_0 < 0$) generated by a preload spring to prevent tensile deformations of the piezoceramic, and δ_V the change in length due to the applied voltage V. The change in length δ_V induced by the applied voltage is given by

$$\delta_V = nl\, d_{33}(V/t) \tag{2}$$

where l is the length of the actuator, n the number of piezoelectric layers, d_{33} a coefficient for the piezoelectric material, and t the thickness of each layer.

In this work, the layout of the active element (i.e., n, d_{33}, and t) is taken from Ref. 4. The control voltage in Eq. (2) is

Received June 26, 1992; revision received March 19, 1993; accepted for publication April 8, 1993.

*Assistant Professor, Mechanical, Aerospace, and Nuclear Engineering. Member AIAA.

†Postdoctoral Research Associate, Mechanical, Aerospace, and Nuclear Engineering; currently Senior Researcher, Korea Aerospace Research Institute. Member AIAA.

‡Rockwell Professor of Aerospace Engineering, Emeritus. Fellow AIAA.

determined by a direct output feedback control law in which elastic change in length δ and time rate of elastic change in length $\dot{\delta}$ (for active elements) are fed back to the controller. The control law is then characterized by the corresponding relative displacement and velocity gains, which are considered as independent design variables.

Mathematical Modeling

The (0,1) formulation of the optimal placement problem makes use of a variable α that indicates the presence (1) or absence (0) of an active element at a given location. For the mathematical model, two elements in parallel, one passive and one active, are initially introduced at each location where an active element may be placed. For the structural model, these two elements are combined in what will be denoted as a hybrid element. The hybrid element properties are obtained by adding the active element properties multiplied by α and the passive element properties multiplied by $(1-\alpha)$. The equivalent mechanical stiffness for the hybrid element is then given by

$$k_h = \alpha k_a + (1-\alpha)k_p \tag{3}$$

where

$$k_a = E_a A_a / l \tag{4a}$$

is the stiffness of active element and

$$k_p = E_p A_p / l \tag{4b}$$

is the stiffness of passive element where E_a and A_a are the equivalent Young's modulus and area of the active element; E_p and A_p are the Young's modulus and area of the passive element; and l is the length of the hybrid element. In the same way, the equivalent mass of the hybrid element is given by

$$m_h = \alpha m_a + (1-\alpha)m_p \tag{5}$$

where the mass of active element

$$m_a = \rho_a A_a l \tag{6a}$$

and the mass of passive element

$$m_p = \rho_p A_p l \tag{6b}$$

and ρ_a is the equivalent mass density of the active elements, and ρ_p is the mass density of the passive elements.

Since the two elements are in parallel, the force in the hybrid element is given by

$$F_h = \alpha F_a + (1-\alpha)F_p \tag{7}$$

Substituting the expression for F_a given by Eq. (1) into Eq. (7) and replacing F_p by $k_p\delta$ gives

$$F_h = \alpha k_a(\delta + \delta_0 - \delta_V) + (1-\alpha)k_p\delta \tag{8}$$

or

$$F_h = [\alpha k_a + (1-\alpha)k_p]\delta + \alpha k_a\delta_0 - \alpha k_a\delta_V \tag{9}$$

Substituting k_h from Eq. (3) into Eq. (9) gives

$$F_h = k_h\delta + \alpha k_a\delta_0 - \alpha k_a\delta_V \tag{10}$$

Finally, relating δ_V and the applied voltage V using Eq. (2) gives

$$F_h = k_h\delta + \alpha k_a\delta_0 - \alpha k_a\gamma V \tag{11}$$

where

$$\gamma = nld_{33}/t \tag{12}$$

To design the control law, the applied voltage V in Eq. (11) is written in the form

$$V = V_0 + V_R \tag{13}$$

where V_0 is a reference voltage and V_R the control voltage to be determined according to a feedback control law. The total voltage V has to be positive to avoid depolarization of the piezoelectric materials.[4] By introducing the positive reference voltage V_0, the total voltage remains positive regardless of the sign of the control voltage V_R (provided that $|V_R| \le V_0$).

Sensors can be built into the active elements to effectively measure the elastic change in length of the actuator (see Refs. 3-5). This information is then used to generate a feedback control law for the control voltage V_R. For a collocated direct output feedback control law, V_R is given by

$$V_R = h_d\delta + h_v\dot{\delta} \tag{14}$$

where h_d and h_v are the gains associated with relative displacement δ and relative velocity $\dot{\delta}$. Introducing Eqs. (13) and (14) into Eq. (11), the expression for the hybrid element force is given by

$$F_h = k_h\delta - \alpha k_a\gamma h_d\delta - \alpha k_a\gamma h_v\dot{\delta} + \alpha k_a\delta_0 - \alpha k_a\gamma V_0 \tag{15}$$

From the previous expression it is seen that the gains h_d and h_v provide stiffness and damping augmentation (k_A and c_A) in the closed-loop system, that is,

$$k_A = \alpha k_a\gamma h_d \tag{16a}$$

$$c_A = \alpha k_a\gamma h_v \tag{16b}$$

Structural/Control System Description

Using a finite element representation of the structure and assuming that for dynamic analysis purposes δ and $\dot{\delta}$ for active elements are measured from the reference configuration given after the voltage V_0 is applied, the dynamic system equations of motion can be written as

$$[M]\{\ddot{q}(t)\} + [C_A]\{\dot{q}(t)\} + [K_A]\{q(t)\} = \{f(t)\} \tag{17}$$

where $[M]$, $[C_A]$, and $[K_A]$ are the $N \times N$ mass, augmented damping, and augmented stiffness matrices, respectively; $\{q(t)\}$ is the $N \times 1$ degree-of-freedom vector; $\{f(t)\}$ is the $N \times 1$ vector of external disturbances; and N is the total number of degrees of freedom for the finite element model of the structure.

The mass of the active elements is considered in the mass matrix by assembling the equivalent mass for hybrid elements given by Eq. (5). The damping matrix $[C_A]$ includes only the damping augmentation provided by the active elements [see Eq. (16b)] and the augmented stiffness includes the passive stiffness and stiffness augmentation for hybrid elements [see Eqs. (3) and (16a)] as well as the stiffness of truss elements.

A transient response analysis of the structure, subject to general time-dependent external loading, would require numerical integration using some type of time-stepping technique. To avoid an expensive time-stepping analysis procedure, in this work attention is limited to transient loads applied during some specified time interval $[t_0, t_1]$. It is then assumed that for $t > t_1$ the structure is not subject to external loads. Furthermore, it is assumed that during the time interval $[t_0, t_1]$ the external loads can be represented by a truncated Fourier series of the form

$$\{f(t)\} = \sum_n (\{f_{nc}\}\cos\Omega_n t + \{f_{ns}\}\sin\Omega_n t) \tag{18}$$

For this class of loading, closed-form transient analysis can be carried out and high quality explicit approximations for peak

transient displacements and peak transient control forces can be constructed (see Appendix).

In the static case, the equations of motion reduce to

$$[K]\{q_s\} = \{f_s\} \tag{19}$$

where the subscript s is used to indicate static displacements and loads. In this case, the stiffness matrix is assembled using the stiffness for hybrid elements given by Eq. (3).

Problem Statement

Qualitatively, the structural/control synthesis problem can be stated as follows: seek a design (Y^*, α^*) which minimizes some measure of system performance subject to the condition that all of the appropriate measures of system behavior and all of the continuous design variables remain within prescribed bounds. The foregoing problem statement can be quantified by formulating it as a general nonlinear mathematical programming problem of the form

$$\begin{aligned} &\text{Min} && f(Y, \alpha) \\ &\text{subject to} && g_j(Y, \alpha) \le 0 && j = 1, \ldots, m \\ &&& \underline{Y}_i \le Y_i \le \bar{Y}_i && i = 1, \ldots, n_C \\ &&& \alpha_k = 0 \text{ or } 1 && k = 1, \ldots, n_D \end{aligned} \tag{20}$$

where m is the number of constraints, n_C the number of continuous variables, and n_D the number of (0,1) variables.

Behavior constraints for the problem stated in Eq. (20) can include static stress, static displacement, closed-loop damping ratios, steady-state and peak transient dynamic displacements, as well as constraints associated with the piezoelectric actuators. In practice the piezoceramic in the actuator should not experience any tensile stress (or force). This restriction is accommodated by introducing precompression δ_0 of the piezoelectric material. Since F_a can still be positive, depending on the elastic deformation δ and the deformation due to applied voltage δ_V [see Eq. (1)], constraints are imposed directly on Eq. (1), namely,

$$F_a = k_a(\delta + \delta_0 - \delta_V) \le 0 \tag{21}$$

After substituting the expression for δ_V from Eq. (2), and V and V_R from Eqs. (13) and (14), the preceding equation results in

$$\delta - \gamma(h_d\delta + h_v\dot{\delta}) + \delta_0 - \gamma V_0 \le 0 \tag{22}$$

Control voltages V_R are also constrained such that the applied voltage V remains in the range $0 \le V \le V_{\max} = 2V_0$, which in view of Eq. (13) is equivalent to

$$-V_0 \le V_R \le V_0 \tag{23}$$

or from Eq. (14)

$$-V_0 \le h_d\delta + h_v\dot{\delta} \le V_0 \tag{24}$$

The dynamic compression constraints given by Eq. (22) and the control voltage constraints given by Eq. (24) are imposed for steady-state and transient loads.

Other constraints considered for practical implementation include 1) lower and upper bounds on the number of active elements and 2) joint constraints such that at specified nodes some concurrent elements cannot be active simultaneously. These are linear constraints in terms of the (0,1) variables. For example, the joint constraints can be written as follows:

$$\sum_{i \in I_j} \alpha_i \le 1 \tag{25}$$

where I_j represents the set corresponding to indexes of possible active elements meeting at joint j.

The objective function options considered in this work include structural mass, control effort, and dynamic displacement at specific locations.

The design optimization problem represented by Eqs. (20) is highly nonlinear, and the objective function and the constraints are complicated implicit functions of the design variables. Therefore, direct application of a nonlinear programming algorithm for its solution is computationally impractical even for small systems. A more tractable approach is to replace the solution of this implicit nonlinear problem by the solution of a sequence of explicit approximate problems in which only the critical and potentially critical constraints are retained and move limits are used to protect the approximations. In this context, the presence of (0,1) variables introduces nondifferentiability of the various functions with respect to these variables. This difficulty is overcome by the use of branch and bound techniques, where at each stage the discrete variables remain continuous within 0-1 bounds.

Branch and bound strategies consist of solving a tree of continuous relaxations of the original discrete problem until a feasible optimal discrete solution is achieved. The vertices of the tree correspond to a problem where a subset of the discrete variables are held fixed at their bounds and the remaining discrete variables are allowed to be continuous between 0 and 1. These vertices are arranged into levels in the following way: There is a single vertex at level 0 (called the root of the tree) which corresponds to the complete continuous relaxation of the original problem. Subsequent levels are generated by choosing a discrete variable α_i and generating two vertices for which α_i has the value 0 for the first node and 1 for the second node. Therefore, a partition of the discrete set is generated where only a subset of the discrete variables are relaxed (i.e., allowed to be continuous).

In this work a simplification of the classical branch and bound strategy is adopted.[13] In this context, the complete relaxation of the problem (root node) is first solved using a sequence of approximate problems. This first phase in the solution procedure is called the continuous screening phase. From the solution obtained, those (0,1) variables that are near

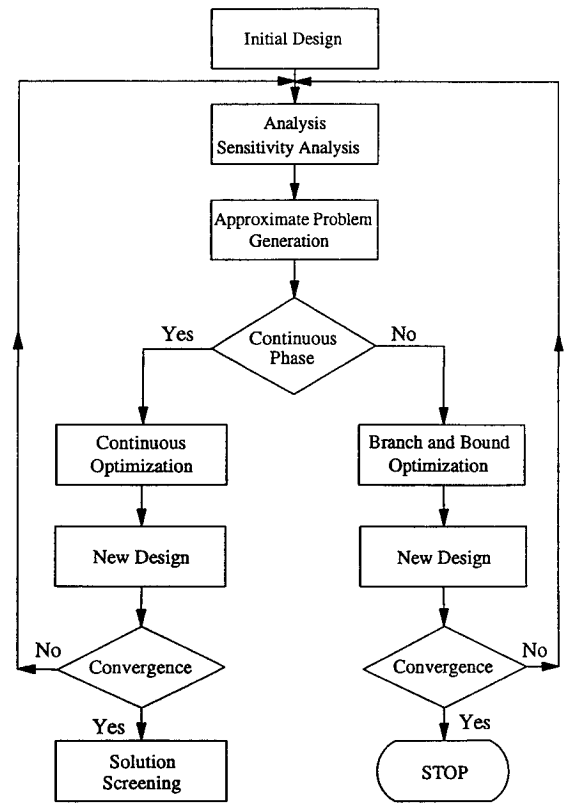

Fig. 1 Block diagram of the design optimization procedure.

0 or 1 are rounded off to 0 or 1 and eliminated from the set of design variables. Then, to find the optimal (0,1) values of the discrete variables that remain after screening, a new sequence of approximate problems is solved using branch and bound. For details on the implementation of branch and bound algorithms see Ref. 14. It should be noted that the branch and bound strategy adopted in this work is more efficient than classical branch and bound since it is only applied to the approximate problem, where all of the necessary functions are explicit. Figure 1 shows the basic steps in the design procedure that has been implemented.

Approximate Problem Generation

In seeking robust approximations of behavior constraints (and objective functions), it is important to appreciate the flexibility offered by the use of intermediate design variables and intermediate response quantities. These ideas originally introduced in Ref. 15 have recently been applied with considerable success to approximations for natural frequencies,[16] static stresses,[17] complex eigenvalues,[18] steady-state displacements,[19] and transient peak displacements.[20]

For the successful implementation of the idea of intermediate response quantities, it is essential to find a set of appropriate intermediate design variables. These intermediate design variables should be chosen such that the first-order approximations of the intermediate response quantities are of high quality with respect to these intermediate design variables.

In this work, the actual design variables are the area A_p for each passive element and A_a, h_d, and h_v for each active element and the (0, 1) variables α. An examination of Eqs. (4), (6), and (15) reveals that the key matrices involved in both static and dynamic analyses (i.e., $[M]$, $[K]$, $[K_A]$, $[C_A]$) are linear functions of the following variables (for hybrid elements):

$$X_1 = \frac{\alpha E_a A_a}{l} + (1-\alpha)\frac{E_p A_p}{l} \tag{26a}$$

$$X_2 = [\alpha \rho_a A_a + (1-\alpha)\rho_p A_p]l \tag{26b}$$

$$X_3 = \left(\frac{E_a \gamma}{l}\right)\alpha A_a h_d \tag{26c}$$

$$X_4 = \left(\frac{E_a \gamma}{l}\right)\alpha A_a h_v \tag{26d}$$

These variables are chosen in this work as intermediate design variables for hybrid elements, and the areas for truss elements are used directly as design variables. Complex eigenvalues, dynamic steady-state and peak transient displacements, and peak transient voltages are approximated using the complex modal energies T_i, S_i, and U_i (see Appendix). These intermediate response quantities are approximated in terms of intermediate design variables, using first-order information.

Numerical Examples

The control augmented structural synthesis methodology described previously has been implemented in a research computer program which is operational on the IBM 3090 computer at the University of California, Los Angeles. The continuous optimization phase was implemented using DOT,[21] and the branch and bound phase was developed using routines from DOC.[22]

Test Problem

An 18-bar truss problem drawn from Ref. 23 was used as a test problem. This problem was solved using continuous optimization as well as the discrete approach described in this paper. For all of the cases the results, in terms of placement and optimal weight, were essentially the same as those reported in Ref. 23. A detailed comparison of these test problem results with those drawn from Ref. 23 will be found in Ref. 24.

Precision Truss Example Problem

The precision truss shown in Fig. 2 has been studied previously at the Jet Propulsion Laboratory (JPL).[3-5] The JPL precision truss is a six-bay truss structure with two opposing outriggers on the top bay. The base of the structure is held fixed. There is a 10-lb weight attached to the end of each outrigger and a 2.5-lb weight attached to each corner of the middle level of the truss. A 10-lb rigid plate is attached to the middle level of the truss. There are also 0.18-lb connectors located at each joint. Node numbers are shown in Fig. 2, and each element will be identified by the two end node numbers. The truss members are composed of aluminum with a density of 0.1 lb/in.^{3} and a Young's modulus of 10^7 lb/in.^{2}. The piezoelectric active elements have a stiffness of $k_a = 23.3 \times 10^3$ lb/in., a weight of 0.556 lb, $\gamma = 4.37 \times 10^{-6}$ in./V, and precompression $\delta_0 = 6 \times 10^{-3}$ in. The reference voltage V_0 is preassigned to be 500 V, and the operational range of V is constrained to the interval $0 \le V \le 1000$ V.

Possible locations for the active elements are any of the members below the midplate, excluding horizontal members (24 locations). To preclude the possibility of control elements acting against one another, special constraints are included to prevent two or more active elements from meeting at a joint. Move limits between 20 and 90% are used throughout this example problem. The load is applied at a point that is located one-quarter of the way between the corner and the midpoint of the plate in the yz plane as shown in Fig. 2, so as to cause both bending and torsional motion of the structure.

Case 1: Dynamic Displacement Minimization

In this case the design objective is to minimize the summation of steady-state displacements of the two outriggers (nodes 41 and 42) in the y and z directions when the truss is subjected to a harmonic load (with a magnitude of 7.07 lb at a frequency of 12.0 Hz) applied to the mid-plate as shown in Fig. 2.

Two runs are made for this case. In the first run, three active elements are placed at locations 11-12, 21-2, and 22-23 ($\alpha = 1$) and all of the other elements are passive ($\alpha = 0$); therefore, this run involves no discrete variables. These fixed locations are the same as those selected in Ref. 3. Active members have fixed areas ($A_a = 0.8$ in.^{2}), and the initial gain values are $h_d = -2 \times 10^5$ V/in. and $h_v = 500$ V · s/in. with side constraints of -2×10^5 V/in. $\le h_d \le 10^6$ V/in. and $0 \le h_v \le 10^6$ V · s/in. The areas of all of the passive members are fixed at

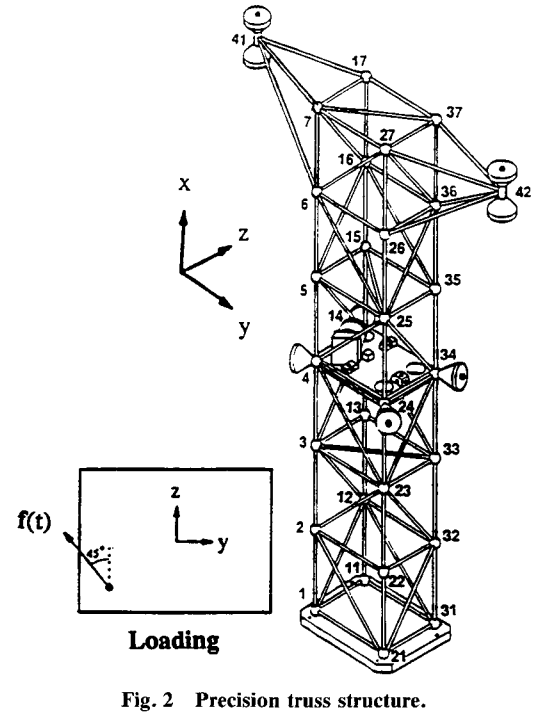

Fig. 2 Precision truss structure.

$A_p = 0.02$ in.^{2} Thus, in run 1 the actual design variables are h_d and h_v for three prepositioned active elements. Constraints are imposed on the damping ratios of the first two complex modes ($11\% \le \xi_1 \le 90\%$ and $4\% \le \xi_2 \le 90\%$). Voltage constraints ($|V_R| \le 500$ V) and nontension constraints are also considered for the active elements. In the second run α are used as design variables in addition to the gains. All of the elements for the possible active member locations have the same initial design variable values, namely, $\alpha = 0.5$, $h_d = -2 \times 10^5$ V/in., and $h_v = 500$ V · s/in., and the same fixed areas as in the first run. For the second run, joint constraints that prevent two or more active elements from meeting at a node are included and the number of active elements is constrained to be between two and three.

Iteration histories are plotted in Fig. 3 and final gains for active elements are given in Table 1. The first run converges to a final objective of 0.0717 in. after seven analyses. For all of the iteration history plots, open markers represent iterations in the continuous screening phase, and solid markers represent iterations in the branch and bound phase. In the second run, after the continuous screening phase elements 21-22 and 31-32 are rounded off to be active ($\alpha = 1$), elements 1-2 and 11-12 are left undecided, and all of the other elements are rounded off to be passive ($\alpha = 0$). After five branch and bound iterations, the design converges to the objective value of 0.0632 in., with three active elements at locations 11-12, 21-22, and 31-32. In both runs the lower bound damping ratio constraint ($\xi_2 \ge 4\%$) is active at the final design, and in the second run the upper bound constraint on the number of active elements is also active.

Case 2: Control Effort Minimization

Case 2 is similar to case 1 except that the design objective is now control effort, which is defined as the summation of the steady-state control forces. Dynamic displacements at the outriggers are constrained to be less than or equal to 1.0 in the y and z directions.

The first run has the same three fixed active elements as in run 1 of case 1 and in the second run α are also design variables. Iteration histories and final gains of active elements are given in Fig. 4 and Table 2, respectively. In the second run element 31-32 is rounded off to be active ($\alpha = 1$), elements 11-12 and 2-3 are left undecided (two discrete variables), and all of the others are rounded off to be passive ($\alpha = 0$). In the final design element 2-3 in addition to element 31-32 becomes active. In both runs lower bound constraints on the first damping ratio are active, and in the second run the second damping ratio constraint and number of active elements constraint are also active at their lower bounds. The final objective function value in run 1 (three fixed location active elements) is 25.11 lb, and it is decreased to 19.14 lb in run 2 (24% reduction with only two active elements).

Table 1 Final gains, precision truss dynamic displacement minimization, case 1

Run 1			Run 2		
Element number	$h_d \times 10^3$, V/in.	$h_v \times 10^3$, V · s/in.	Element number	$h_d \times 10^3$, V/in.	$h_v \times 10^3$, V · s/in.
11-12	−200	1.1507	11-12	−200	3.5612
21-2	−200	0.1758	21-22	−200	0.0727
22-23	−200	1.1610	31-32	−200	0.0823
Objective function, in.	0.07170			0.06317	
Number of analyses	7			16	

Table 2 Final gains, precision truss control effort minimization, case 2

Run 1			Run 2		
Element number	$h_d \times 10^3$, V/in.	$h_v \times 10^3$, V · s/in.	Element number	$h_d \times 10^3$, V/in.	$h_v \times 10^3$, V · s/in.
11-12	−200	1.9424	31-32	−188.19	1.5873
21-2	−13.626	0.2434	2-3	−29.988	2.6943
22-23	−106.49	1.1435			
Objective function, lb	25.11			19.14	
Number of analyses	16			15	

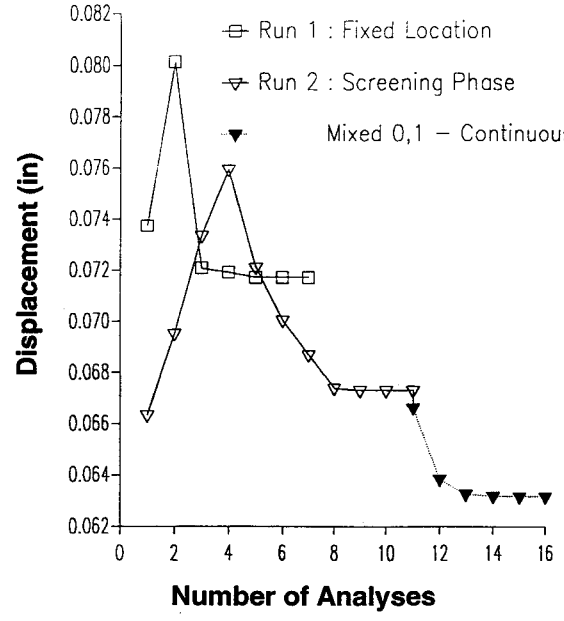

Fig. 3 Iteration histories, precision truss dynamic displacement minimization.

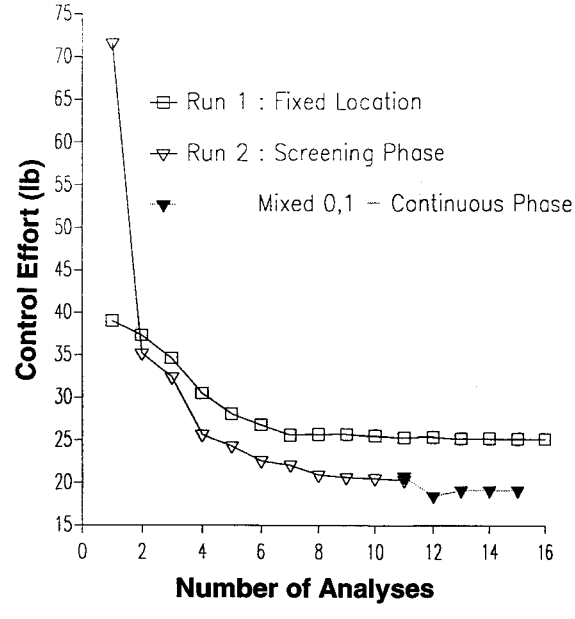

Fig. 4 Iteration histories, precision truss control effort minimization.

Case 3: Weight Minimization I

The objective function in this case is the total weight of the system (i.e., active elements and passive members, excluding all nonstructural masses). The design variables are 1) the areas of passive members with side constraints such that 0.001 in.$^2 \le A_p \le 0.8$ in.^{2}; 2) the gains for the active members with

Table 3 Final passive areas, precision truss weight minimization I, case 3

Element number	$A_p \times 10^{-6}$ in^2 Run 1	Run 2	Run 3	Run 4	Run 5	Element number	Run 1	Run 2	Run 3	Run 4	Run 5
4-5	10,174	9,462	10,848	11,985	10,722	27-37	5,693	10,636	1,475	3,338	1,838
14-15	10,064	10,301	11,904	12,019	14,357	6-41	4,231	7,639	5,696	5,189	5,122
24-25	12,755	14,601	16,039	13,155	16,861	16-41	5,418	8,111	6,066	6,363	5,772
34-35	6,659	6,225	8,924	7,943	8,215	7-41	4,846	8,637	2,957	3,586	3,531
4-25	5,172	9,452	5,649	3,418	4,491	17-41	4,138	8,013	3,159	2,504	3,840
14-5	8,725	11,313	6,647	8,656	7,276	26-42	3,980	7,645	4,703	3,833	4,279
14-35	4,966	6,760	8,669	5,756	5,554	36-42	3,917	8,073	1,965	1,799	2,466
34-25	6,344	10,634	5,034	3,850	4,385	27-42	4,677	8,631	1,104	1,858	2,092
5-15	5,742	10,704	1,003	3,312	1,680	37-42	4,490	8,284	5,641	4,506	5,457
5-25	4,650	9,251	1,177	2,331	1,001	2-12	5,561	10,580	1,006	3,167	1,000
15-25	4,797	8,995	1,242	2,633	2,631	2-22	4,605	9,229	1,000	2,324	1,065
15-35	4,974	9,561	1,136	2,720	2,285	12-32	4,595	9,227	1,000	2,324	1,067
25-35	5,599	10,598	1,000	3,169	1,001	22-32	5,560	10,579	1,000	3,167	1,000
5-6	8,325	10,585	2,825	2,379	3,493	3-13	5,531	10,566	1,001	3,204	1,495
15-16	10,069	10,306	11,680	12,023	14,348	3-23	4,611	9,232	1,000	2,326	1,198
25-26	7,499	8,621	8,989	7,492	7,619	13-23	3,939	8,331	1,012	2,238	2,264
35-36	7,674	11,920	4,196	2,614	5,066	13-33	4,527	9,200	1,000	2,452	1,763
5-16	6,590	9,197	6,116	6,853	6,435	23-33	5,567	10,582	1,620	3,168	1,000
25-6	6,898	11,599	6,402	5,449	5,100	1-2	7,344	7,762	2,151	6,923	10,686
25-36	5,669	9,804	5,916	4,198	5,390	1-12	4,560	8,008	1,014	1,028	2,777
35-16	6,251	8,013	8,731	7,328	5,356	21-32	4,972	8,725	5,375	4,386	1,120
6-16	5,646	10,623	1,651	3,364	2,231	31-12	4,208	9,597	4,213	4,536	5,086
6-26	4,792	9,342	2,997	3,383	4,302	12-13	11,376	9,303	6,838	10,042	11,553
16-36	4,940	9,492	1,131	2,336	2,237	32-33	3,579	9,365	10,903	5,895	5,531
26-36	5,634	10,618	1,009	3,231	1,002	2-23	3,094	10,670	1,025	1,494	1,445
6-7	4,961	9,346	1,993	3,057	4,247	12-3	4,567	8,003	1,000	1,022	3,926
16-17	4,695	9,292	1,001	2,298	1,146	12-33	4,208	9,593	4,149	4,487	5,298
26-27	6,493	8,701	6,016	5,265	5,689	32-23	4,944	8,725	5,542	4,383	2,518
36-37	4,712	8,510	5,321	5,473	5,780	3-4	5,284	10,920	4,657	2,772	1,514
6-27	6,736	8,889	3,054	3,988	2,962	13-14	11,382	9,308	7,601	10,101	12,266
16-7	4,587	8,560	2,960	3,054	4,087	23-24	5,442	9,853	12,937	8,422	4,713
16-37	5,065	6,047	7,155	7,481	7,506	23-4	3,847	9,500	1,579	1,570	2,665
36-27	4,856	9,076	4,108	3,138	4,382	23-34	7,179	9,829	5,671	4,342	2,681
7-17	5,664	10,610	1,826	3,360	2,809	33-14	3,424	8,602	5,607	4,914	6,333
7-27	5,346	9,553	2,876	3,729	3,584	21-22	15,003	8,091	15,750	11,386	6,966
17-27	4,235	8,501	1,182	2,083	2,562	2-3	4,036	6,126	4,389	4,467	7,731
17-37	4,768	9,274	1,064	2,488	2,378	3-14	4,248	9,129	1,668	2,926	2,343

Table 4 Final design, precision truss weight minimization I, case 3

Element number	Design variables	Run 1	Run 2	Run 3	Run 4	Run 5
11-12	α	1	1	1	1	1
	$A_p \times 10^{-6}$ in.^{2}	—	—	—	—	—
	$h_d \times 10^3$ V/in.	−200	−200	−185.5	−198.868	−199.93
	$h_v \times 10^3$ V · s/in.	1.1569	0.8659	1.1367	0.6810	1.1663
31-32	α	0	1	1	1	0
	$A_p \times 10^{-6}$ in.^{2}	10,808	—	—	—	1,000
	$h_d \times 10^3$ V/in.	—	−178.06	−199.68	−198.74	—
	$h_v \times 10^3$ V · s/in.	—	1.0746	1.2181	0.7888	—
21-2	α	1	1	0	0	0
	$A_p \times 10^{-6}$ in.^{2}	—	—	1,756	1,556	1,291
	$h_d \times 10^3$ V/in.	−115.24	−167.04	—	—	—
	$h_v \times 10^3$ V · s/in.	0.9488	0.8102	—	—	—
22-23	α	1	0	0	0	0
	$A_p \times 10^{-6}$ in.^{2}	—	8,093	14,934	11,522	6,835
	$h_d \times 10^3$ V/in.	−200	—	—	—	—
	$h_v \times 10^3$ V · s/in.	0.8188	—	—	—	—
33-34	α	0	0	1	0	0
	$A_p \times 10^{-6}$ in.^{2}	5,986	9,969	—	2,981	4,133
	$h_d \times 10^3$ V/in.	—	—	−97.007	—	—
	$h_v \times 10^3$ V · s/in.	—	—	0.4329	—	—
Final weight, lb		2.259	2.609	2.138	1.590	1.031
Number of analyses		10	16	23	18	20

the same side constraints used in cases 1 and 2; and 3) the (0,1) variables for the 24 possible locations.

Five runs are made for this example. In all of these runs, the steady-state dynamic loading used in case 1 is applied. The displacements of the outriggers are constrained to be $|q_y| \leq 0.01$ in. and $|q_z| \leq 0.03$ in. The damping ratios for the first three modes are constrained to be $\xi_1 \geq 11\%$, $\xi_2 \geq 4\%$, and $\xi_3 \geq 1\%$. The control effort is constrained to be less than or equal to 20 lb.

Iteration histories and final designs are given in Fig. 5 and Tables 3 and 4. Table 3 reports the final areas for truss elements and the passive areas of hybrid elements which turn out to be passive in all five runs. Table 4 shows the final designs of the elements that are active in at least one of these five runs. In the first two runs, active member locations are fixed. In the first run (fixed locations A) locations 11-12, 21-2, and 22-23 are chosen according to Ref. 3. The optimal weight for this run is 2.259 lb. In the second run (fixed locations B) locations 11-12, 31-32, and 21-2 are chosen since intuitively one expects the most effective actuator locations to be near the base of the structure. However, the optimum weight for this run is 2.609 lb indicating that the three fixed locations used in Ref. 3 give a better result.

In runs 3–5 the α are (0,1) design variables. In run 3, the number of actuators is constrained to be greater than or equal to 3. At the end of the continuous screening phase, 13 discrete variables remain to be decided by the branch and bound optimization phase. The optimal weight obtained is 2.138 lb with active element locations 11-12, 31-32, and 33-34. By treating the placement variables α as design variables, the objective function is reduced by about 5% compared to the fixed locations (fixed locations A). For the fourth run, the lower bound on the number of active elements is relaxed to two. At the end of the continuous screening phase the number of undecided (0,1) variables is five. The optimal weight is now reduced to 1.590 lb with active element locations 11-12 and 31-32. This result shows that two active elements are sufficient to control the first three modes and satisfy all of the behavior constraints considered. It should be noted that the reduction in the final weight is due primarily to the fact that one of the

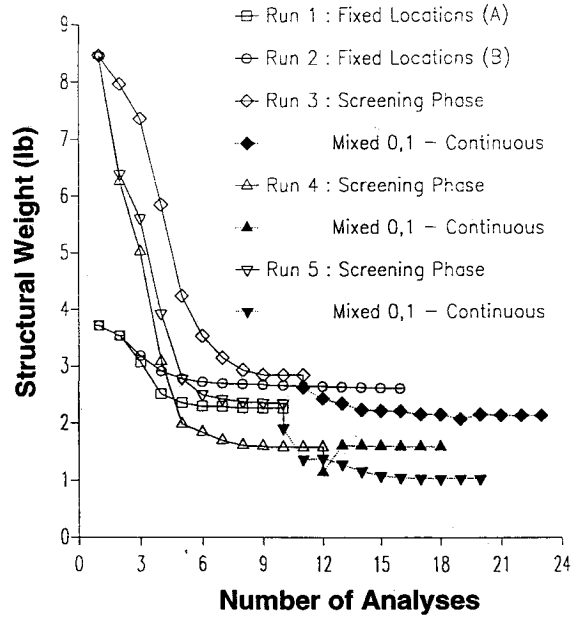

Fig. 5 Iteration histories, precision truss weight minimization I.

Table 5 Final design, precision truss weight minimization II, case 4

Element number	$A_p \times 10^{-6}$ in^2 Run 1	Run 2	Run 3	Run 4	Element number	Run 1	Run 2	Run 3	Run 4
4-5	16,026	17,717	12,385	10,353	27-37	16,661	17,721	7,759	11,582
14-15	9,383	10,248	6,559	4,644	6-41	15,296	16,098	5,107	6,232
24-25	9,383	9,684	11,569	7,754	16-41	15,223	15,002	3,381	5,946
34-35	12,274	13,306	17,461	8,473	7-41	15,263	16,210	2,214	7,712
4-25	15,106	18,461	14,383	9,192	17-41	14,282	15,776	5,070	7,693
14-5	17,329	16,723	11,024	8,322	26-42	12,474	15,850	8,813	5,756
14-35	12,111	15,315	10,886	7,038	36-42	14,622	16,403	7,422	6,563
34-25	16,469	19,878	10,349	11,494	27-42	15,681	16,571	5,604	8,830
5-15	16,645	17,562	13,362	9,649	37-42	13,028	15,773	5,030	6,767
5-25	15,280	16,721	8,571	9,289	2-12	16,368	17,563	5,365	11,508
15-25	15,532	15,867	7,379	8,498	2-22	15,106	16,640	11,190	9,223
15-35	15,813	16,556	7,476	9,823	12-32	15,089	16,637	11,461	8,710
25-35	16,471	17,606	10,848	11,459	22-32	16,365	17,562	10,809	11,658
5-6	15,738	15,956	2,967	15,333	3-13	16,420	17,588	14,618	11,992
15-16	9,383	10,321	9,167	6,397	3-23	15,133	16,651	7,209	8,997
25-26	9,383	13,409	9,321	9,012	13-23	14,488	16,082	2,805	7,622
35-36	16,756	21,022	8,384	15,583	13-33	15,238	16,703	8,897	9,289
5-16	16,557	16,691	10,883	7,901	23-33	16,360	17,571	16,093	11,503
25-6	16,022	17,886	12,351	10,794	1-2	14,581	12,905	9,241	7,250
25-36	13,782	19,288	8,889	10,215	1-12	14,288	15,790	2,122	7,138
35-16	13,094	17,305	13,558	6,098	21-32	16,312	18,257	9,758	10,573
6-16	16,584	17,678	10,437	9,335	31-12	21,679	19,264	17,722	9,641
6-26	14,758	17,051	9,946	9,190	12-13	14,067	13,488	16,478	7,727
16-36	15,635	17,225	9,511	9,543	32-33	9,352	16,636	22,931	17,165
26-36	16,527	17,665	12,806	11,295	2-23	23,300	19,769	6,301	6,095
6-7	15,944	16,990	10,224	7,904	12-3	17,367	15,584	7,324	7,131
16-17	15,461	16,853	9,850	9,258	12-33	21,377	18,949	12,012	8,721
26-27	11,930	14,280	8,222	9,328	32-23	15,886	18,252	8,306	10,412
36-37	12,687	15,121	11,901	8,806	3-4	19,208	20,222	8,650	6,522
6-27	14,910	13,921	4,562	9,806	13-14	14,807	11,557	10,756	11,387
16-7	15,499	16,488	13,219	7,744	23-24	17,036	16,771	12,642	9,870
16-37	10,384	11,226	7,929	6,639	23-4	20,949	17,909	6,398	7,796
36-27	14,523	17,801	6,528	8,849	23-34	21,683	18,651	8,264	10,772
7-17	16,653	17,729	4,395	11,644	33-14	18,249	18,673	12,104	7,062
7-27	15,931	16,845	3,648	9,243	21-22	18,293	10,560	10,230	11,277
17-27	14,881	16,482	3,431	7,671	2-3	9,389	11,082	4,196	6,210
17-37	15,147	16,816	3,415	8,276	33-34	19,730	19,442	10,071	13,224

three active elements could be eliminated by using the optimization methodology that has been developed. For the fifth run, no lower bound on the number of actuators is imposed. Five (0,1) variables are left undecided at the end of the continuous screening phase. The final solution involves a single actuator at position 11-12 and the optimal weight is 1.031 lb. Thus, it is seen that by proper placement of the appropriate number of active element(s) the minimum mass can be reduced by more than a factor of 2.

Case 4: Weight Minimization II

Case 4 is the same weight minimization problem as in case 3 except that in this case additional transient behavior constraints ($|q_y(t)| \leq 0.01$ in. and $|q_z(t)| \leq 0.03$ in. at the outriggers) are considered due to a transient half-sine pulse with amplitude of 7.07 lb and with frequency of 12 Hz (i.e., the load is applied during the time interval $0 \leq t \leq 0.0417$ s). This pulse is applied at the same point and in the same direction on the midplate (see Fig. 2). Transient responses are considered for the time period of $0 \leq t \leq 1$ s, and 12 complex modes are used for the truncated transient response calculation.

In the first two runs the previously used fixed locations for active elements are considered (run 1 and run 2 in case 3). In run 3, the minimum number of active elements to be selected is constrained to be 3. Run 4 is identical to run 3 except that no constraint on the minimum number of active elements is imposed.

Iteration histories and final design information are given in Fig. 6 and Tables 5 and 6. The first two runs converge to designs with similar final weights (3.249 and 3.342 lb). In run 3 after the continuous screening phase, eight discrete variables remain to be decided by the branch and bound algorithm. The final weight obtained in this run is 2.592 lb which is lower than the fixed location results by more than 20% with three active elements at 11-12, 31-32, and 3-14. In the final run (run 4), seven (0,1) variables are left undecided at the end of the continuous screening phase. The final weight is now reduced to 2.032 lb with two active elements at 11-12 and 31-32. In all of the runs, transient displacements of both outriggers in the y direction are active. In run 2 the third damping ratio is active, in run 3 the control effort and the first damping ratio constraints are active, and in run 4 control effort as well as the first and the second damping ratio constraints are active (at the final designs).

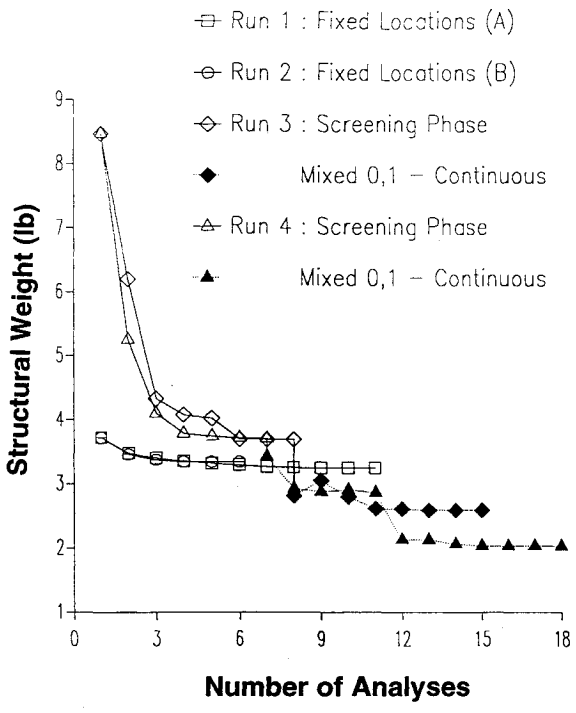

Fig. 6 Iteration histories, precision truss weight minimization II.

Table 6 Final design, precision truss weight minimization II, case 4

Element number	Design variables	Run 1	Run 2	Run 3	Run 4
11-12	α	1	1	1	1
	$A_p \times 10^{-6}$ in.^{2}	—	—	—	—
	$h_d \times 10^3$ V/in.	−200	−199.59	−185.13	−188.77
	$h_v \times 10^3$ V · s/in.	1.2009	0.9172	1.9578	2.0772
31-32	α	0	1	1	1
	$A_p \times 10^{-6}$ in.^{2}	12,744	—	—	—
	$h_d \times 10^3$ V/in.	—	−199.55	−195.00	−200
	$h_v \times 10^3$ V · s/in.	—	0.9543	1.2578	1.2822
21-2	α	1	1	0	0
	$A_p \times 10^{-6}$ in.^{2}	—	—	1,179	5,955
	$h_d \times 10^3$ V/in.	−200	−198.82	—	—
	$h_v \times 10^3$ V · s/in.	0.6976	0.8910	—	—
22-23	α	1	0	0	0
	$A_p \times 10^{-6}$ in.^{2}	—	10,540	14,818	11,411
	$h_d \times 10^3$ V/in.	−184.85	—	—	—
	$h_v \times 10^3$ V · s/in.	0.9005	—	—	—
3-14	α	0	0	1	0
	$A_p \times 10^{-6}$ in.^{2}	18,340	17,963	—	6,399
	$h_d \times 10^3$ V/in.	—	—	−151.33	—
	$h_v \times 10^3$ V · s/in.	—	—	1.5906	—
Final weight, lb		3.249	3.342	2.592	2.032
Number of analyses		11	6	15	18

Conclusions

A synthesis methodology for the design of control augmented structures modeled as an assemblage of truss elements and active control elements has been presented. Areas for structural elements; (0,1) variables for active element placement; and areas, position gains, and velocity gains for active elements are independent design variables for the synthesis problem.

The design problem is posed as a nonlinear mixed (0,1)-continuous mathematical programming problem. The objective function options considered include the sum of the velocity gains, dynamic displacement, total weight, and control effort. Constraints on dynamic steady-state and transient response, control voltage, number of active elements, and closed-loop eigenvalues are considered as well as nontension and joint constraints. The mixed (0,1)-continuous design problem is solved by combining approximation concepts and branch and bound techniques. High quality approximations are constructed using intermediate response quantities and intermediate design variables.

The results demonstrate the effectiveness of the design optimization procedure outlined in Fig. 1. The branch and bound techniques combined with approximation concepts are found to be efficient. The final designs reported here are obtained using a relatively small number of actual analyses (10-23). Introducing hybrid elements to formulate the active member placement problem facilitates the selection of appropriate intermediate design variables [see Eqs. (26)]. The generality of the nonlinear programming formulation [see Eq. (20)] makes it possible to incorporate novel but important constraints such as: the voltage constraints [see Eqs. (23) and (24)]; the nontension requirements for the active elements [see Eqs. (21) and (22)]; various joint constraints designed to prevent concurrency of active elements [Eq. (25)]; and limitations on the total number of active elements.

Appendix: Equations for Intermediate Response Quantities

Complex Eigenvalues (Ref. 18)

The second-order eigenvalue problem associated with the equations of motion stated in Eq. (17) is given by

$$\{\lambda^2[M] + \lambda[C_A] + [K_A]\}\{\phi\} = \{0\} \tag{A1}$$

For collocated sensor-actuator pairs the matrices $[M]$, $[C_A]$, and $[K_A]$ are symmetric. Premultiplying Eq. (A1) by $\{\phi\}^T$ and solving for λ gives

$$\lambda = \sigma \pm i\omega_d = \frac{-S \pm \sqrt{S^2 - 4UT}}{2T} \tag{A2}$$

where

$$U = \{\phi\}^T[K_A]\{\phi\} \tag{A3a}$$

$$T = \{\phi\}^T[M]\{\phi\} \tag{A3b}$$

$$S = \{\phi\}^T[C_A]\{\phi\} \tag{A3c}$$

The eigenvalues given by Eq. (A2) appear in complex conjugate pairs. The quantities U, T, and S are chosen as intermediate response quantities and are approximated to first order in terms of the intermediate design variables [Eqs. (26)], assuming that the eigenvectors remain invariant. The damping ratio is then evaluated as

$$\xi = \frac{-\sigma}{\sqrt{\sigma^2 + \omega_d^2}} \tag{A4}$$

Steady-State Response (Ref. 19)

From Eq. (17) assuming a harmonic load of the form

$$\{f(t)\} = \{f_0\}e^{i\Omega t} \tag{A5}$$

and using the complex eigenvectors [see Eq. (A1)] to decouple the system, the steady-state dynamic displacement is given by

$$\{q(t)\} = \{q_0\}e^{i\Omega t} \tag{A6}$$

where

$$\{q_0\} = \{A_R\} + i\{A_I\} \tag{A7a}$$

$$\{A_R\} = 2Re\left(\sum_{j=1}^{n} \frac{\lambda_j\{\phi_j\}^T\{f_0\}}{(\Omega^2 + \lambda_j^2)(2\lambda_j T_j + S_j)}\{\phi_j\}\right) \tag{A7b}$$

$$\{A_I\} = 2\Omega Re\left(\sum_{j=1}^{n} \frac{\{\phi_j\}^T\{f_0\}}{(\Omega^2 + \lambda_j^2)(2\lambda_j T_j + S_j)}\{\phi_j\}\right) \tag{A7c}$$

The intermediate response quantities U_j, T_j, and S_j are approximated in terms of intermediate design variables. From these approximations and assuming that the complex eigenvectors are invariant, the complex quantities λ_j and in turn $\{A_k\}$ and $\{A_I\}$ are obtained using Eqs. (A2), (A7b), and (A7c).

From the approximate displacements, the control forces and control voltages are easily obtained from Eqs. (14) and (15).

Transient Response (Ref. 20)

The time-dependent load is assumed to be represented by a truncated Fourier series as shown in Eq. (18). Using a modal analysis, the dynamic displacements can be written as

$$\{q(t)\} = Re\sum_{j=1}^{n}\left\{\{\phi_j\}\left[\left(\frac{\lambda_j TV_j + TD_j}{1+\lambda_j^2} - \eta_j(t_0)\right)e^{\lambda_j(t-t_0)} + \eta_i(t)\right]\right\} \tag{A8}$$

where

$$\eta_j(t) = \sum_r (a_{jr}\sin\Omega_r t + b_{jr}\cos\Omega_r t) \tag{A9a}$$

$$a_{jr} = \frac{\lambda_j(-\lambda_j\{\phi_j\}^T\{f_{rs}\} + \Omega_r\{\phi_j\}^T\{f_{rc}\})}{(1+\lambda_j^2)(\lambda_j^2 + \Omega_r^2)} \tag{A9b}$$

$$b_{jr} = \frac{\lambda_j(-\Omega_r\{\phi_j\}^T\{f_{rs}\} - \lambda_j\{\phi_j\}^T\{f_{rc}\})}{(1+\lambda_j^2)(\lambda_j^2 + \Omega_r^2)} \tag{A9c}$$

$$TV_j = \{\phi_j\}^T[M]\{\dot{q}(t_0)\} \tag{A9d}$$

$$TD_j = \{\phi_j\}^T[M]\{q(t_0)\} \tag{A9e}$$

The intermediate response quantities for this case are U_j, T_j, S_j, TV_j, and TD_j. The transient dynamic constraints are imposed at peak times, and these times are assumed invariant for each approximate problem.

Acknowledgment

The sponsorship provided by the NASA Langley Research Center under Grant NASA NSG-1490 is gratefully acknowledged.

References

[1]Nurre, G. S., Ryan, R. S., Scofield, H. N., and Sims, J. L., "Dynamics and Control of Large Space Structures," *Journal of Guidance, Control, and Dynamics,* Vol. 7, No. 5, 1984, pp. 514-526.

[2]Rodriguez, G. (ed.), *Proceedings of the Workshop on Identification and Control of Flexible Structures,* Jet Propulsion Lab., JPL Pub. 85-29, Pasadena, CA, April 1985, Vols. I-III.

[3]Fanson, J. L., Blackwood, G. H., and Chu, C.-C., "Active-Member Control of Precision Structures," *Proceedings of the AIAA/ASME/ASCE/AHS/ASC 30th Structures, Structural Dynamics, and Materials Conference* (Mobile, AL), AIAA, Washington, DC, 1989, pp. 1480-1494 (AIAA Paper 89-1329).

[4]Anderson, E. H., Moore, D. M., Fanson, J. L., and Ealey, M. A., "Development of an Active Member Using Piezoelectric and Electrostrictive Actuation for Control of Precision Structures," *Proceedings of the AIAA/ASME/ASCE/AHS/ASC 31st Structures, Structural Dynamics, and Materials Conference* (Long Beach, CA), AIAA, Washington, DC, 1990, pp. 2221-2233 (AIAA Paper 90-1085).

[5]Fanson, J. L., and Garba, J. A., "Experimental Studies of Active Members in Control of Large Space Structures," *Proceedings of the AIAA/ASME/ASCE/AHS/ASC 29th Structures, Structural Dynamics, and Materials Conference* (Williamsburg, VA), AIAA, Washington, DC, 1988, pp. 9-17 (AIAA Paper 88-2207).

[6]Salama, M., Bruno, R., Chen, G. S., and Garba, J., "Optimal Placement of Excitations and Sensors by Simulated Annealing," *Proceedings of the Second NASA/Air Force Symposium on Recent Advances in Multidisciplinary Analysis and Optimization* (Hampton, VA), NASA Office of Management, Scientific and Technical Information Div., Washington, DC, 1988, pp. 1441-1457.

[7]Chiu, D., and Skelton, R. E., "Selecting Measurements and Controls in LQG Problems," *Proceedings of the 20th IEEE Conference on Decision and Control* (San Diego, CA), Inst. of Electrical and Electronics Engineers, New York, 1981, pp. 491-494.

[8]Chang, I. J., and Soong, T. T., "Optimal Controller Placement in Model Control of Complex Systems," *Journal of Mathematical Analysis and Applications,* Vol. 75, No. 2, 1980, pp. 340-358.

[9]Horner, G. C., "Optimum Damper Locations for Structural Vibration Control," *Proceedings of the AIAA/ASME/ASCE/AHS Structures, Structural Dynamics, and Materials Conference* (New Orleans, LA), AIAA, Washington, DC, 1982, pp. 29-45 (AIAA Paper 82-0635).

[10]Horner, G. C., "Optimum Actuator Placement, Gain, and Number for a Two-Dimensional Grillage," *Proceedings of the AIAA/ASME/ASCE/AHS Structures, Structural Dynamics, and Materials Conference* (Lake Tahoe, NV), AIAA, Washington, DC, 1983, pp. 179-184 (AIAA Paper 83-0854).

[11]Haftka, R. T., "Optimum Placement of Controls for Static Deformations of Space Structures," *AIAA Journal,* Vol. 22, No. 9, 1984, pp. 1293-1298.

[12]Haftka, R. T., and Adelman, H. M., "Effect of Sensor and Actuator Errors on Static Shape Control for Large Space Structures," *AIAA Journal,* Vol. 25, No. 1, 1987, pp. 134-138.

[13]Sepulveda, A. E., and Schmit, L. A., "Optimal Placement of Actuators and Sensors in Control Augmented Structural Optimization," *International Journal for Numerical Methods in Engineering,* Vol. 32, No. 6, 1991, pp. 1165-1187.

[14]Sherali, H. D., and Myers, D. C., "The Design of Branch and Bound Algorithms for a Class of Nonlinear Integer Programs," *Journal of Operations Research,* Vol. 5, No. 6, 1985, pp. 463-484.

[15]Schmit, L. A., and Miura, H., "Approximation Concepts for Efficient Structural Synthesis," NASA CR 2552, March 1976.

[16]Canfield, R. A., "An Approximation Function for Frequency Constrained Structural Optimization," *Proceedings of the Second NASA/Air Force Symposium on Recent Advances in Multidisci-*

plinary Analysis and Optimization (Hampton, VA), NASA Office of Management, Scientific and Technical Information Div., Washington, DC, 1988, pp. 937–953.

[17]Vanderplaats, G. N., and Salajegheh, E., "A New Approximation Method for Stress Constraints in Structural Synthesis," *AIAA Journal,* Vol. 27, No. 3, 1989, pp. 352–358.

[18]Thomas, H. L., Sepulveda, A. E., and Schmit, L. A., "Improved Approximations for Control Augmented Structural Optimization," *AIAA Journal,* Vol. 30, No. 1, 1992, pp. 171–179.

[19]Thomas, H. L., Sepulveda, A. E., and Schmit, L. A., "Improved Approximations for Dynamic Displacements using Intermediate Response Quantities," *Proceedings of the 3rd Air Force/NASA Symposium on Recent Advances in Multidisciplinary Analysis and Optimization* (San Francisco, CA), Wright Lab., Wright-Patterson AFB, OH, 1990, pp. 95–104.

[20]Sepulveda, A. E., Thomas, H. L., and Schmit, L. A., "Improved Transient Response Approximations for Control Augmented Structural Optimization," *Proceedings of the Second Pan American Congress of Applied Mechanics* (Valparaiso, Chile), Wright Lab., Wright-Patterson AFB, OH, 1991, pp. 611–614.

[21]Vanderplaats, G. N., and Hansen, S. R., DOT Users Manual, Version 2.04, VMA Engineering, Goleta, CA, 1989.

[22]Vanderplaats, G. N., and Hansen, S. R., DOC Users Manual, Version 1.00, VMA Engineering, Goleta, CA, 1991.

[23]Horta, L. G., Juang, J. N., and Junkins, J. L., "A Sequential Linear Optimization Approach for Controller Design," *Journal of Guidance, Control, and Dynamics,* Vol. 9, No. 6, 1986, pp. 699–703.

[24]Sepulveda, A. E., Jin, I. M., and Schmit, L. A., "Optimal Placement of Active Elements in Control Augmented Structural Synthesis," *Proceedings of the AIAA/ASME/AHS/ASC 33rd Structures, Structural Dynamics, and Materials Conference* (Dallas, TX), AIAA, Washington, DC, 1992 (AIAA Paper 92-2557).